

## Single-neutron orbits near $^{78}\text{Ni}$ : Spectroscopy of the N=49 isotope $^{79}\text{Zn}$

R. Orlandi, D. Mucher, R. Raabe, A. Jungclaus, S.D. Pain, V. Bildstein, R. Chapman, G. De Angelis, J.G. Johansen, P. Van Duppen, et al.

► **To cite this version:**

R. Orlandi, D. Mucher, R. Raabe, A. Jungclaus, S.D. Pain, et al.. Single-neutron orbits near  $^{78}\text{Ni}$ : Spectroscopy of the N=49 isotope  $^{79}\text{Zn}$ . Physics Letters B, Elsevier, 2014, 740, pp.298-302. 10.1016/j.physletb.2014.12.006 . in2p3-01093962

**HAL Id: in2p3-01093962**

**<http://hal.in2p3.fr/in2p3-01093962>**

Submitted on 5 Jan 2015

**HAL** is a multi-disciplinary open access archive for the deposit and dissemination of scientific research documents, whether they are published or not. The documents may come from teaching and research institutions in France or abroad, or from public or private research centers.

L'archive ouverte pluridisciplinaire **HAL**, est destinee au depot et à la diffusion de documents scientifiques de niveau recherche, publies ou non, emanant des tablissements d'enseignement et de recherche franais ou trangers, des laboratoires publics ou privs.



## Single-neutron orbits near $^{78}\text{Ni}$ : Spectroscopy of the $N = 49$ isotope $^{79}\text{Zn}$



R. Orlandi<sup>a,b,c,d,e,\*</sup>, D. Mücher<sup>f</sup>, R. Raabe<sup>b</sup>, A. Jungclaus<sup>a</sup>, S.D. Pain<sup>g</sup>, V. Bildstein<sup>f</sup>, R. Chapman<sup>c,d</sup>, G. de Angelis<sup>h</sup>, J.G. Johansen<sup>i</sup>, P. Van Duppen<sup>b</sup>, A.N. Andreyev<sup>c,d,j,e</sup>, S. Bottoni<sup>b,k</sup>, T.E. Cocolios<sup>m</sup>, H. De Witte<sup>b</sup>, J. Diriken<sup>b</sup>, J. Elseviers<sup>b</sup>, F. Flavigny<sup>b</sup>, L.P. Gaffney<sup>n,b</sup>, R. Gernhäuser<sup>f</sup>, A. Gottardo<sup>h</sup>, M. Huyse<sup>b</sup>, A. Illana<sup>a</sup>, J. Konki<sup>l,o,p</sup>, T. Kröll<sup>q</sup>, R. Krücken<sup>f</sup>, J.F.W. Lane<sup>c,d</sup>, V. Liberati<sup>c,d</sup>, B. Marsh<sup>r</sup>, K. Nowak<sup>f</sup>, F. Nowacki<sup>s</sup>, J. Pakarinen<sup>l,o,p</sup>, E. Rapisarda<sup>b</sup>, F. Recchia<sup>t</sup>, P. Reiter<sup>u</sup>, T. Roger<sup>b,v</sup>, E. Sahin<sup>h</sup>, M. Seidlitz<sup>u</sup>, K. Sieja<sup>s</sup>, J.F. Smith<sup>c,d</sup>, J.J. Valiente Dobón<sup>h</sup>, M. von Schmid<sup>q</sup>, D. Voulot<sup>r</sup>, N. Warr<sup>u</sup>, F.K. Wenander<sup>r</sup>, K. Wimmer<sup>f</sup>

<sup>a</sup> Instituto de Estructura de la Materia, IEM-CSIC, Madrid, E-28006, Spain

<sup>b</sup> KU Leuven, Instituut voor Kern- en Stralingsfysica, B-3001 Heverlee, Belgium

<sup>c</sup> School of Engineering, University of the West of Scotland, Paisley, PA1 2BE, United Kingdom

<sup>d</sup> Scottish Universities Physics Alliance (SUPA), United Kingdom

<sup>e</sup> Advanced Science Research Center, Japan Atomic Energy Agency, Tokai, Ibaraki, 319-1195, Japan

<sup>f</sup> Physik Department E12, Technische Universität München, D-85748 Garching, Germany

<sup>g</sup> Physics Division, Oak Ridge National Laboratory, Oak Ridge, TN 37831, USA

<sup>h</sup> Istituto Nazionale di Fisica Nucleare, Laboratori Nazionali di Legnaro, Legnaro, I-35020, Italy

<sup>i</sup> Department of Physics and Astronomy, Aarhus University, DK-8000 Aarhus, Denmark

<sup>j</sup> Department of Physics, University of York, Heslington, YO10 5DD, United Kingdom

<sup>k</sup> Dipartimento di Fisica, Università di Milano and INFN Sezione di Milano, I-20133, Italy

<sup>l</sup> PH Department, CERN 1211, Geneva 23, Switzerland

<sup>m</sup> School of Physics and Astronomy, University of Manchester, Manchester, M13 9PL, United Kingdom

<sup>n</sup> Oliver Lodge Laboratory, University of Liverpool, Liverpool L69 9ZE, United Kingdom

<sup>o</sup> Helsinki Institute of Physics, University of Helsinki, P.O. Box 64, FIN-00014 Helsinki, Finland

<sup>p</sup> Department of Physics, University of Jyväskylä, P.O. Box 35, FIN-40014 Jyväskylä, Finland

<sup>q</sup> Institut für Kernphysik, Technische Universität Darmstadt, D-64289 Darmstadt, Germany

<sup>r</sup> AB Department, CERN 1211, Geneva 23, Switzerland

<sup>s</sup> IPHC, CNRS/IN2P3, Université de Strasbourg, F-67037 Strasbourg, France

<sup>t</sup> Università degli studi di Padova and INFN Sezione di Padova, Padova I-35131, Italy

<sup>u</sup> Institut für Kernphysik, Universität zu Köln, D-50937 Köln, Germany

<sup>v</sup> GANIL, CEA/DSM-CNRS/IN2P3, F-14076 Caen, France

### ARTICLE INFO

#### Article history:

Received 5 October 2014

Received in revised form 18 November 2014

Accepted 3 December 2014

Available online 9 December 2014

Editor: D.F. Geesaman

#### Keywords:

Nuclear structure

$\gamma$ -Ray transitions

Transfer reactions

$N = 50$  shell closure

### ABSTRACT

Single-neutron states in the  $Z = 30$ ,  $N = 49$  isotope  $^{79}\text{Zn}$  have been populated using the  $^{78}\text{Zn}(d,p)^{79}\text{Zn}$  transfer reaction at REX-ISOLDE, CERN. The experimental setup allowed the combined detection of protons ejected in the reaction, and of  $\gamma$  rays emitted by  $^{79}\text{Zn}$ . The analysis reveals that the lowest excited states populated in the reaction lie at approximately 1 MeV of excitation, and involve neutron orbits above the  $N = 50$  shell gap. From the analysis of  $\gamma$ -ray data and of proton angular distributions, characteristic of the amount of angular momentum transferred, a  $5/2^+$  configuration was assigned to a state at 983 keV. Comparison with large-scale-shell-model calculations supports a robust neutron  $N = 50$  shell-closure for  $^{78}\text{Ni}$ . These data constitute an important step towards the understanding of the magicity of  $^{78}\text{Ni}$  and of the structure of nuclei in the region.

© 2014 The Authors. Published by Elsevier B.V. This is an open access article under the CC BY license (<http://creativecommons.org/licenses/by/3.0/>). Funded by SCOAP<sup>3</sup>.

\* Corresponding author at: Advanced Science Research Center, Japan Atomic Energy Agency, Tokai, Ibaraki, 319-1195, Japan.

E-mail address: [orlandi.riccardo@jaea.go.jp](mailto:orlandi.riccardo@jaea.go.jp) (R. Orlandi).

Shell structure characterizes several many-body systems of fermions moving in a common potential, such as atomic electrons, metal clusters and nuclei. Angular momentum quantization induces a bunching of the single-particle states, resulting in shells separated by energy gaps. In the nuclear medium, such shell gaps are revealed by nuclei with neutron and proton numbers corresponding to closed-shell configurations. The properties of these so-called magic nuclei and of their neighbors, which were cardinal to the development of the nuclear shell model, could only be reproduced when the role played by the nuclear spin-orbit interaction was recognized [1].

In recent years, experiments with radioactive ion beams have shown that in some neutron-rich nuclei well-established shell closures can vanish, and new magic numbers appear [2,3]. The challenge to explain and predict the size of shell gaps away from beta stability has led to considerable progress in nuclear physics, both experimentally and theoretically. Despite some remarkable steps forward in describing the evolution of shell structure, e.g. the inclusion of the tensor interaction [4] and three-body forces [5,6], rare-isotope data are still essential to test and guide theoretical advances. Nuclei away from the valley of beta stability with magic numbers of neutrons and protons, and isotopes in their vicinity, have become new cornerstones for the development of a reliable theoretical picture of all nuclei.

The region of isotopes near  $^{78}\text{Ni}$  is the focus of intense experimental and theoretical research (cf., for example, [7–12] and references therein). Whether  $^{78}\text{Ni}$  can be considered a doubly-magic spherical nucleus depends ultimately on the size of the  $Z = 28$  and  $N = 50$  shell gaps. To date, however, scarce information is available on  $^{78}\text{Ni}$  and on its immediate neighbors, and contrasting predictions have been made [12,13] about its magicity.

The properties of nuclei lying close to  $^{78}\text{Ni}$  also impact strongly on astrophysical models of stellar nucleosynthesis and evolution. A recent example is related to the measurement of the  $^{82}\text{Zn}$  binding energy and its implications on the composition of neutron-star crust [14]. Furthermore, a sensitivity study on the effect of neutron-capture rates on the  $A \sim 80$  and  $A \sim 130$  r-process peaks [15] revealed that  $^{78}\text{Zn}$  and  $^{79}\text{Zn}$  are among the few isotopes which can cause the largest change ( $>15\%$ ) in the overall abundance pattern, affecting the abundances of masses as high as  $A \sim 195$ .

Single-nucleon transfer reactions are a very sensitive technique to populate single-particle states and to investigate the structure of the isotopes produced [16–19]. Performing such reactions on  $^{78}\text{Ni}$  will reveal the energies of the single-particle orbits governing the properties of  $^{78}\text{Ni}$  and its neighbors. The necessary experiments however still require years of developments in radioactive-ion-beam production. Revealing insights about the structure of  $^{78}\text{Ni}$  can nonetheless be gained by studying close-lying isotopes. Moreover, an accurate description of the evolution of nuclear structure across neighboring nuclei is an implicit test for theoretical predictions of the properties of  $^{78}\text{Ni}$ .

In this Letter, the first spectroscopic study of the  $Z = 30$ ,  $N = 49$  isotope  $^{79}\text{Zn}$  is presented. In this nucleus, neutrons can occupy orbits which lie both below and above the  $N = 50$  shell gap. Prior to this work, the available information about  $^{79}\text{Zn}$  was limited to its ground-state half life, 0.995(19) s [20]. The beta decay of  $^{79}\text{Zn}$  [8] supports a  $J^\pi = 9/2^+$  ground-state configuration, in line with the shell-model expectation that the odd neutron (hole) occupies the  $g_{9/2}$  orbit, and with  $N = 49$  systematics. In the present work, the  $9/2^+$  assignment for the ground state has been adopted.

In this work, excited states in  $^{79}\text{Zn}$  have been populated using the  $^{78}\text{Zn}(d,p)^{79}\text{Zn}$  reaction in inverse kinematics at REX-ISOLDE, CERN (Q value = 1.796 MeV [21]).  $^{78}\text{Zn}$  ( $T_{1/2} = 1.47(15)$  s) was produced in collisions of 1.4 GeV protons from the CERN PS Booster

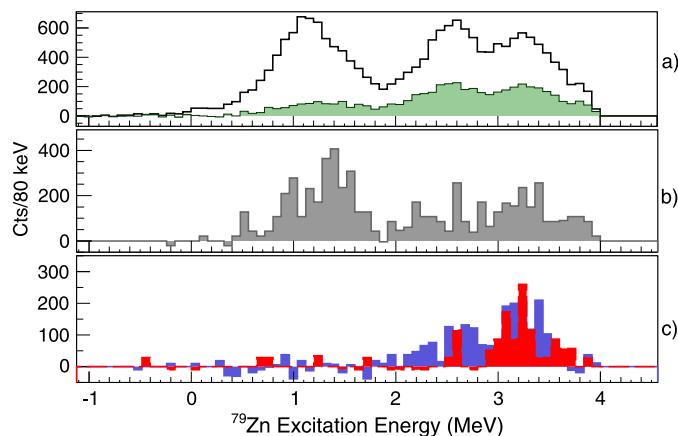


**Fig. 1.** (Color online.) a)  $^{79}\text{Zn}$  excitation energy deduced from proton kinematics for all the transfer protons (black solid line) and from the protons in coincidence with any  $\gamma$  ray (green, solid fill). b)  $^{79}\text{Zn}$  excitation energy in coincidence with the 983-keV  $\gamma$  ray, corrected for  $\gamma$ -ray efficiency. c) Same as b), but in coincidence either with the 236-keV (blue) or the 1859-keV  $\gamma$  transitions (red).

with a  $\text{UC}_x$  target.  $^{78}\text{Zn}$  atoms were laser ionized using the RILIS set up [22], mass separated, and post-accelerated by the REX-LINAC to 2.83 MeV per nucleon. The  $^{78}\text{Zn}$  beam impinged on a thin ( $105(10)$   $\mu\text{g}/\text{cm}^2$ ) deuterated polyethylene (DPE) target. In addition to  $^{78}\text{Zn}$ , which made up  $\sim 75\%$  of the total intensity, the beam also contained  $^{78}\text{Rb}$  ( $\sim 20\%$ ) and  $^{78}\text{Ga}$  ( $\sim 5\%$ ). Exploiting the fact that without laser ionization only  $^{78}\text{Zn}$  disappeared from the beam cocktail, the contribution from the contaminants could be identified and subtracted offline by collecting data with the laser periodically turned on and off (in total, approximately 100 hours with and 35 hours without laser ionization). From the analysis of elastically scattered deuterons, the estimated average  $^{78}\text{Zn}$  beam intensity was  $7.8(7) \cdot 10^5$  particles per second. Additional data (approximately 20 hours), collected using a thick ( $\sim 1.7$   $\text{mg}/\text{cm}^2$ ) DPE target, permitted to confirm weak coincidences observed in the thin-target data.

The reaction was studied using the segmented T-REX array of Si telescopes [23], and eight triple-cluster HPGe detectors of Miniball [24], which surrounded the T-REX scattering chamber. The coincident detection of light charged particles and  $\gamma$  rays led to the identification of states which could not be resolved using only the proton data. Furthermore, the charged-particle data constrained the placement of states in the level scheme which would have been ambiguous from the  $\gamma$ -ray data alone.

In Fig. 1 (a), the  $^{79}\text{Zn}$  excitation energy deduced from reaction kinematics is shown for proton singles and protons in coincidence with all detected  $\gamma$  rays. Three main peaks can be seen, centered respectively around 1.2, 2.5 and 3.3 MeV. Due to kinematic compression and to the detection threshold, only transfer protons corresponding to the lowest-energy peak could be detected both at forward and backward angles, and meaningfully compared to DWBA calculations. At this beam energy, the transferred neutrons should populate mainly states or groups of states corresponding to low- $\ell$  orbits, mostly above the  $N = 50$  gap, namely  $d_{5/2}$ ,  $s_{1/2}$  and  $d_{3/2}$ . The  $g_{7/2}$  orbit above the gap ( $\ell = 4$ ) and the neutron-hole states based on  $p$  or  $f$  configuration are likely to be populated very weakly. As an illustration, the  $^{79}\text{Zn}$  case can be compared to the study of the  $N = 81$  isotone  $^{131}\text{Sn}$  via the  $^{130}\text{Sn}(d,p)^{131}\text{Sn}$  reaction [17], in which only neutron orbits above the  $N = 82$  gap were populated.

Fig. 1 (a) reveals that the lowest-lying states which are strongly populated via transfer are found near 1 MeV. This observation is important, since the position of the excited states based on neutron orbits above the  $N = 50$  shell reflects the gap size. As

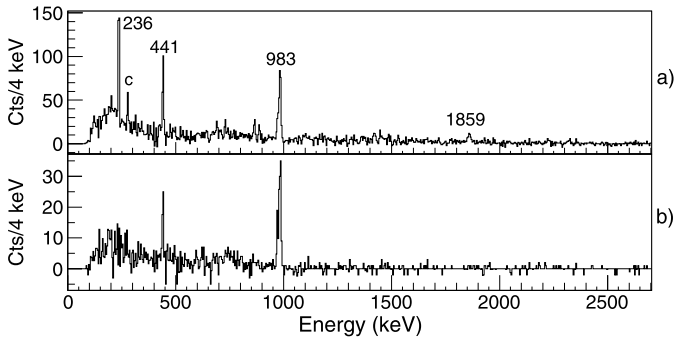


**Fig. 2.** a) Doppler-corrected  $^{79}\text{Zn}$   $\gamma$ -ray spectrum, gated by all transfer protons. The strongest peaks are labeled by their energy. The peak labeled “c” is due to a small amount of  $^{78}\text{Ga}$  in the beam, due to in-flight  $^{78}\text{Zn}$   $\beta$  decay. b) Same spectrum gated on  $^{79}\text{Zn}$  excitation energy in the 0.8–1.7 MeV range, where only the 441- and 983-keV transitions can be seen. See text for details.

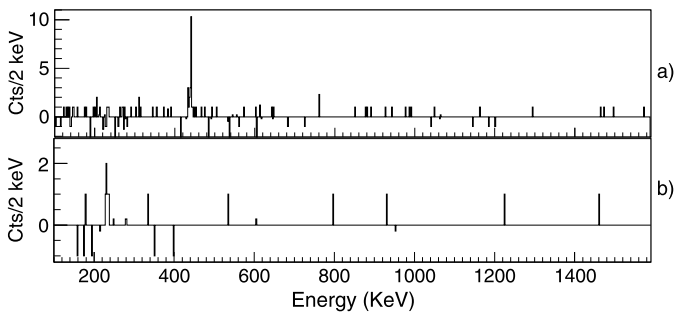


**Fig. 3.** Coincidence  $\gamma$ -ray spectra gated, respectively, on the 983-keV (a) or the 1859-keV (b) transitions, obtained using thick-target data.

discussed below, the analysis of proton angular distributions are indeed consistent with transfer of neutrons to the  $d_{5/2}$  and  $s_{1/2}$  orbits. The green curve in the same figure shows that, in coincidence with  $\gamma$ -rays, the intensity of the first peak decreases significantly more than that of the two higher-lying peaks. This observation suggests the presence, in the excitation-energy range of the first peak, of one or more states which are too long lived (more than few nanoseconds) for their decay(s) to be detected in flight.

The  $\gamma$  rays emitted by  $^{79}\text{Zn}$  were identified by requiring a coincidence with the protons ejected in the neutron-transfer reactions. The Doppler-corrected  $\gamma$ -ray energy spectrum is shown in Fig. 2 (a). Fig. 1 (b) and (c) are examples of excitation-energy spectra of  $^{79}\text{Zn}$  gated by individual  $\gamma$  rays. Similarly, Fig. 2 (b) shows that only the 441- and 983-keV lines are still clearly visible if the  $^{79}\text{Zn}$  excitation energy is restricted to the lowest peak of Fig. 1 (a) (from 0.8 to 1.7 MeV). Such spectra, together with observed  $\gamma$  coincidences, such as those presented in Fig. 3, proved essential to place the main transitions in the level scheme. No other  $\gamma$  ray was observed below 0.8-MeV excitation energy. It should also be noted that the  $\gamma$ -ray detection efficiency drops drastically below 120 keV. Fig. 3 shows that both the 441–983-keV and the 236–1859-keV pairs were each found to be coincident.

The partial level scheme of  $^{79}\text{Zn}$  deduced in this work is presented in Fig. 4. According to measured intensities and coincidence relations, the 983-keV state decays directly to the ground state, and it is fed by the 441-keV transition. Since the 983-keV transition is prompt, despite a low energy tail, its multipolarity can only be dipole or quadrupole. If the tail is due to the lifetime of the 983-keV state, and not to unobserved feeding, it suggests a lifetime of the order of few hundred picoseconds, with multipolarity E2 or M2. A slow E2 ( $0.05 < B(E2) < 0.2$  W.u.) seems much more likely. An M2 character would in fact require this low-lying and strongly populated state to be a  $5/2^-$  state, correspond-

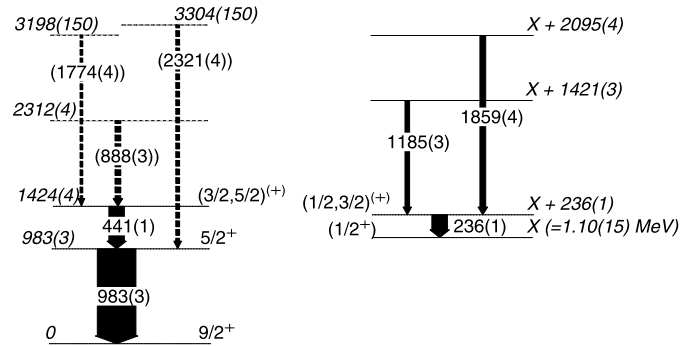


**Fig. 4.** Partial level scheme of  $^{79}\text{Zn}$  deduced in this work. The width of the arrows is proportional to the relative transition intensities. With the exception of the isomeric state ‘X’ at 1.10(15) MeV, all energies are in keV, with the error given in brackets. See text for details.

ing to a neutron-hole in the  $f_{5/2}$  orbit. Interestingly, comparable  $B(E2; 5/2^+ \rightarrow 9/2^+)$  strengths have been measured in neighboring  $N = 49$  isotones  $^{81}\text{Ge}$  and  $^{83}\text{Se}$  (respectively, 0.0383(20) and  $\approx 0.13$  W.u. [25]).

The direct and indirect feeding to the 983-keV state, which makes its ground-state decay the most intense transition in the spectrum, supports a  $5/2^+$  assignment. The DWBA analysis discussed below confirms the  $5/2^+$  assignment deduced from the  $\gamma$ -ray analysis.

In the case of the 1424-keV state, the prompt character of the 441-keV transition, the coincidence between the 983- and 441-keV  $\gamma$  rays and the unobserved crossover ground-state transition favor a spin  $3/2^+$  or  $5/2^+$ . Few additional weak transitions, of 888, 1774 and 2321 keV, were tentatively placed in the level scheme: their  $\gamma$ -ray-gated excitation energy spectra in fact exhibit a peak respectively at 2.35(15), 3.30(15) and 3.45(15) MeV, compatible with a direct feeding to either the 1424- or the 983-keV states. For the 888-keV transition, this placement is also supported by the observed coincidence with the 441-keV transition.

The analysis of the 236- and 1859-keV single- $\gamma$ -ray-gated excitation energy spectra, shown in Fig. 1 (c), is key to positioning the 236-keV transition in the level scheme. A peak at  $\sim 3.20(15)$  MeV can be seen in both spectra (blue and red in the figure), but only the 236-keV gate shows also a peak at 2.65(15) MeV, where the large uncertainty is due to the Si-detector resolution (the thin red peak appearing at 2.6 MeV in the 1859-keV gated spectrum is not statistically significant). Their observed coincidence implies that the 236-keV lies below the 1859-keV  $\gamma$  ray (otherwise no peak could appear also at 2.65 MeV excitation energy). Hence, the 236-keV transition must be the decay of a state with energy at least as low as the difference between the 3.2 MeV excitation energy and the 1859-keV  $\gamma$  ray, i.e. 1.34(15) MeV. In Fig. 1 (c), however, no peak appears around or below 1.3 MeV, which means that the state at  $\sim 1.34$  MeV is not (or too weakly) populated in the direct reaction and only fed from higher-lying states. The prompt character of the 236-keV transition implies that it has E1 or M1 multipolarity. The position of the 1185-keV transition was deduced from its  $\gamma$ -gated excitation energy and the coincidence with the 236-keV  $\gamma$  ray.

From the unobserved coincidence with the 983-keV transition it follows that the 236-keV  $\gamma$  ray feeds an isomeric state lying approximately at 1.10(15) MeV. Proton angular distributions, which are characteristic of the angular momentum transfer,  $\Delta\ell$ , provide a strong argument to identify this 1.10(15)-keV state with a  $1/2^+$  state.

The measured proton angular distributions were compared to DWBA calculations performed with the codes FRESKO [26] and TWOFNR [27] using global optical model potentials from

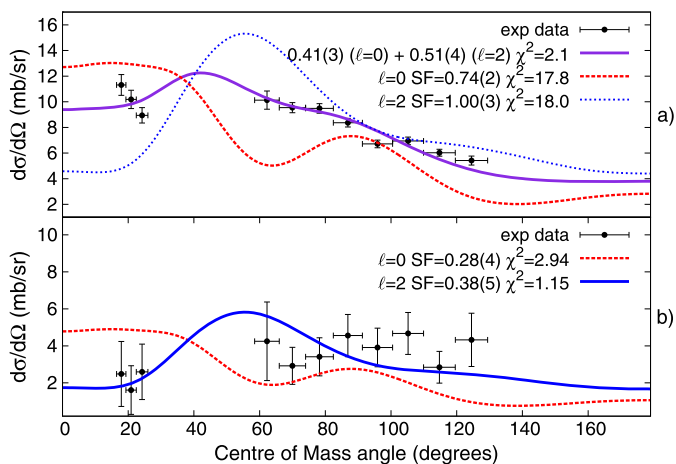


**Fig. 5.** (Color online.) a) Proton angular distributions for the  $^{79}\text{Zn}$  excitation energy range 0.85–1.55 MeV and scaled DWBA calculations for  $\Delta\ell = 0, 2$  and a sum of the two. b) Same proton data, gated also on the 983-keV  $\gamma$ -ray line, and DWBA calculations for  $\Delta\ell = 0$  or 2.

Refs. [28,29]. For the neutron bound-state potential, the radius and diffuseness parameters were 1.25 and 0.65 fm, respectively. Experimental spectroscopic factors (SF) were determined from the ratio of experimental and DWBA cross sections, which were calculated for SF = 1. The low beam energy leads to appreciable differences in the DWBA distributions calculated using different optical-model-potential parameterizations. Additional fits were therefore also performed using different parameters from Refs. [30–33], and varying the bound-state radius parameter from 1.20 to 1.30. The systematic uncertainties amount to approximately 20–25% variation in the calculated SFs. It should be remarked however that the arguments based on the analysis of angular distributions do not depend on the chosen parameterization.

Illustrative angular distributions are shown in Fig. 5 (a) and (b). In both cases, the excitation energy of  $^{79}\text{Zn}$  was restricted to the lowest peak of Fig. 1 (a). The data in Fig. 5 (a) were not gated on any  $\gamma$ -ray line, and are poorly fitted by any single  $\Delta\ell$  transfer. These data are instead well described by a sum of  $\Delta\ell = 0$  and  $\Delta\ell = 2$  distributions. The simultaneous fit of two distributions yields a significantly smaller reduced  $\chi^2$  (2.1) than obtained by fitting a single  $\Delta\ell$  ( $\chi^2 = 17.8$  and 18, respectively). The scaling factors were left as free parameters in the fit and found to be, respectively, 0.41(3)(10) and 0.51(4)(12) (where the first error is statistical, and the second systematic). If, in addition to  $\Delta\ell = 0$  and 2, also a third,  $\Delta\ell = 1$  distribution is added to the simultaneous fit, the latter has a scaling factor compatible with zero while the former are substantially unchanged, indicating that mostly  $d$  and  $s$  orbits were populated in this energy range.

The angular distribution changes instead considerably by requiring the coincident detection of the 983-keV  $\gamma$  ray. This is shown in Fig. 5 (b), together with DWBA calculations for transfer to, respectively, pure  $\ell = 0$  or  $\ell = 2$  states. A pure  $\Delta\ell = 2$  distribution (transfer to a  $d_{5/2}$  or  $d_{3/2}$  neutron state) yields a better fit and confirms the  $5/2^+$  assignment of the 983-keV state deduced from  $\gamma$ -ray data.  $J^\pi = 3/2^+$  can in fact be excluded since it would lead to an isomeric M3 ground-state transition.

A similar distribution is observed when gating the same excitation energy region by the 441-keV transition: the data, not shown here, are best fitted by  $\Delta\ell = 2$ , and yield SF = 0.05(1)(2). The comparison between Fig. 1 (b) and the intensity strength of the 441-keV transition suggests that the 983-keV state is also fed by additional low-energy undetected  $\gamma$ -ray transition(s) from one or more states between 1.0 and 1.4 MeV. The measured angular distributions imply however that these states have  $\ell = 2$  character

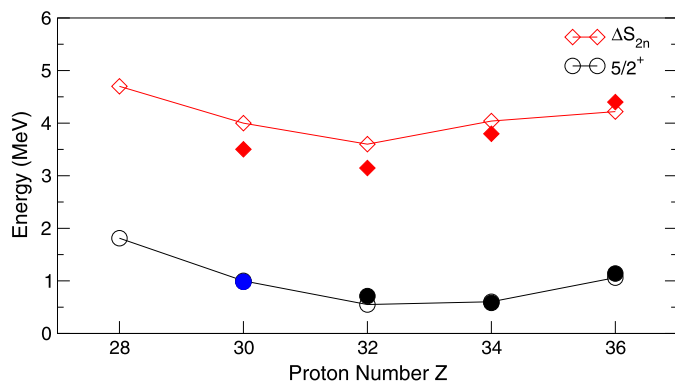


**Fig. 6.** (Color online.) Experimental and calculated  $N = 50$  gap sizes (filled and open diamonds) and first-excited  $5/2^+$ -state energies (filled and open circles) for  $N = 49$  isotones. The measurement from this work is highlighted in blue. The gap sizes were determined from two-neutron separation energies calculated from mass excesses from [21] (and [14] for  $^{82}\text{Zn}$ ).

and feed the 983-keV state. In summary, approximately 75% of the measured  $\ell = 2$  strength in this energy range results in the direct or indirect feeding of the state at 983 keV, again consistent with a  $5/2^+$  assignment.

The  $\Delta\ell = 0$  strength revealed by the proton data (not gated by any  $\gamma$  ray) of Fig. 5 (a) testifies the presence of an isomeric  $1/2^+$  state near 1 MeV, with SF = 0.41(3)(10). The proton-singles data were also split in three smaller ranges in excitation energy and compared to DWBA calculations similar to those in Fig. 5 (a). The weighted average of the  $\ell = 0$  strengths measured in the sub-sets indicates that the  $1/2^+$  state lies at approximately 1.05(15) MeV. It seems likely that this  $s_{1/2}$  neutron state corresponds in fact to the 1.10(15)-MeV state deduced from gamma-ray gated excitation energy spectra (labeled X in Fig. 4). If the strongly populated  $1/2^+$  state coincides indeed with the level at 1.1 MeV, then the prompt observation of the 236-keV  $\gamma$ -ray limits the possible spin of the 1.34(15)-MeV state to  $(1/2)$  or  $(3/2)$  ( $X + 236$  in Fig. 4). The large amount of feeding from higher lying states favors a positive parity, but a negative parity cannot be excluded.

It is instructive to compare the  $5/2^+$ -state energy, 983 keV, with state-of-the-art shell-model calculations [12]. The large shell-model space includes the proton orbits  $p_{1/2}$ ,  $p_{3/2}$ ,  $f_{7/2}$  and  $f_{5/2}$ , and the neutron orbits  $p_{1/2}$ ,  $p_{3/2}$ ,  $f_{5/2}$ ,  $g_{9/2}$  and  $d_{5/2}$ , which lies above the  $N = 50$  shell gap. Details about the interaction can be found in Refs. [12,34]. As it can be seen in Fig. 6, these calculations reproduce very well the measured energies of the lowest lying  $5/2^+$ -state  $N = 49$  isotones. For  $^{79}\text{Zn}$  they predict an energy of 1029 keV, strikingly close to the measured 983 keV. This lowest calculated  $5/2^+$  state (SF = 0.53) is formed by the promotion of one neutron from the  $g_{9/2}$  to the  $d_{5/2}$  orbit. The calculated B(E2) transition strength to the ground state is only  $4 e^2 \text{fm}^4$  (0.2 W.u.). The equivalent lifetime, 240 ps, is compatible with the observed tail of the 983-keV transition.

Fig. 6 shows that the calculations also reproduce reasonably well the evolution of the  $N = 50$  gap deduced from 2-neutron separation energies [14,21], with a minimum at  $Z = 32$  and a larger gap in zinc than in germanium, although the experimental gap size in these two isotones is 450 keV smaller. The calculations predict a doubly-magic  $^{78}\text{Ni}$  with shell gaps of 4.7 MeV for neutrons and 5.0 MeV for protons, and a first  $2^+$ -state lying at nearly 4 MeV. If at least the relative increase in gap size between zinc and nickel is correct, the  $N = 50$  gap in  $^{78}\text{Ni}$  can be expected to be at least as large as 4.2 MeV.

In conclusion, this spectroscopic study of  $^{79}\text{Zn}$  has permitted the identification of key states near 1 MeV of excitation energy,

based on the occupancy of single-particle states above the  $N = 50$  shell gap. The agreement between the current measurement and recent large-scale shell-model calculations supports the picture of a robust  $N = 50$  shell closure for  $^{78}\text{Ni}$ . This newly acquired knowledge about neutron single-particle states in  $^{79}\text{Zn}$  will also be important to constraining neutron-capture rates on  $^{78}\text{Zn}$ , which have been shown to impact the final r-process abundance pattern during freeze-out periods.

## Acknowledgements

This work was supported by the European Commission through the Marie Curie Actions Contracts Nos. PIEFGA-2011-30096 (R.O.) and PIEFGA-2008-219175 (J.P.), by the Spanish Ministerio de Ciencia e Innovación under contracts FPA2009-13377-C02 and FPA2011-29854-C04, by the Spanish MEC Consolider – Ingenio 2010, Project No. CDS2007-00042 (CPAN), by FWO-Vlaanderen (Belgium), by GOA/2010/010 (BOF KU Leuven), by the Interuniversity Attraction Poles Programme initiated by the Belgian Science Policy Office (BriX network P7/12), by the European Union Seventh Framework Programme through ENSAR, contract no. RII3-CT-2010-262010, and by the German BMBF under contracts 05P09PKCI5, 05P12PKFNE, 05P12RDCIA and 06DA9036I. R.O., R.C., J.F.W.L., V.L. and J.F.S. also acknowledge support from STFC, Grant Nos. PP/F000944/1, ST/F007590/1, and ST/J000183/2. The authors thank A.M. Moro for valuable discussions.

## References

- [1] M. Goepfert Mayer, Phys. Rev. 75 (1949) 1969, <http://dx.doi.org/10.1103/PhysRev.75.1969>; O. Haxel, J.H.D. Jensen, H.E. Suess, Phys. Rev. 75 (1949) 1766, <http://dx.doi.org/10.1103/PhysRev.75.1766.2>.
- [2] O. Sorlin, M.-G. Porquet, Prog. Part. Nucl. Phys. 61 (2008) 602, <http://dx.doi.org/10.1016/j.ppnp.2008.05.001>.
- [3] R. Kanungo, Phys. Scr. T 152 (2013) 014002, <http://dx.doi.org/10.1088/0031-8949/2013/T152/014002>.
- [4] T. Otsuka, T. Suzuki, M. Honma, Y. Utsuno, N. Tsunoda, K. Tsukiyama, M. Hjorth-Jensen, Phys. Rev. Lett. 104 (2010) 012501, <http://dx.doi.org/10.1103/PhysRevLett.104.012501>.
- [5] A.P. Zuker, Phys. Rev. Lett. 90 (2003) 042502, <http://dx.doi.org/10.1103/PhysRevLett.90.042502>.
- [6] G. Hagen, M. Hjorth-Jensen, G.R. Jansen, R. Machleidt, T.P. Papenbrock, Phys. Rev. Lett. 109 (2012) 032502, <http://dx.doi.org/10.1103/PhysRevLett.109.032502>.
- [7] Y. Tsunoda, T. Otsuka, N. Shimizu, M. Honma, Y. Utsuno, Phys. Rev. C 89 (2014) 031301(R), <http://dx.doi.org/10.1103/PhysRevC.89.031301>.
- [8] A. Korgul, K.P. Rykaczewski, J.A. Winger, S.V. Ilyushkin, C.J. Gross, et al., Phys. Rev. C 86 (2012) 024307, <http://dx.doi.org/10.1103/PhysRevC.86.024307>.
- [9] Z.Y. Xu, S. Nishimura, G. Lorusso, F. Browne, P. Doornenbal, et al., Phys. Rev. Lett. 113 (2014) 032505, <http://dx.doi.org/10.1103/PhysRevLett.113.032505>.
- [10] T. Marchi, G. de Angelis, T. Baugher, D. Bazin, J. Berryman, EPJ Web Conf. 66 (2014) 02066, <http://dx.doi.org/10.1051/epjconf/20146602066>.
- [11] L. Coraggio, A. Covello, A. Gargano, N. Itaco, Phys. Rev. C 89 (2014) 024319, <http://dx.doi.org/10.1103/PhysRevC.89.024319>.
- [12] K. Sieja, F. Nowacki, Phys. Rev. C 85 (2012) 051301(R), <http://dx.doi.org/10.1103/PhysRevC.85.051301>.
- [13] M.-G. Porquet, O. Sorlin, Phys. Rev. C 85 (2012) 014307, <http://dx.doi.org/10.1103/PhysRevC.85.014307>.
- [14] R.N. Wolf, et al., Phys. Rev. Lett. 110 (2013) 041101, <http://dx.doi.org/10.1103/PhysRevLett.110.041101>.
- [15] R.A. Surman, M.R. Mumpower, G.C. McLaughlin, R. Sinclair, W.R. Hix, K.L. Jones, in: P.E. Garrett, B. Hadinia (Eds.), Proceedings of the 14th International Symposium on Capture Gamma-Ray Spectroscopy and Related Topics, Guelph, 2013, World Scientific, 2013, p. 304.
- [16] K.L. Jones, et al., Nature 465 (2010) 454–457, <http://dx.doi.org/10.1038/nature09048>.
- [17] R.L. Kozub, et al., Phys. Rev. Lett. 109 (2012) 172501, <http://dx.doi.org/10.1103/PhysRevLett.109.172501>.
- [18] J.S. Thomas, et al., Phys. Rev. C 76 (2007) 044302, <http://dx.doi.org/10.1103/PhysRevC.76.044302>.
- [19] D.K. Sharp, et al., Phys. Rev. C 87 (2013) 014312, <http://dx.doi.org/10.1103/PhysRevC.87.014312>.
- [20] K.-L. Kratz, H. Gabelmann, P. Möller, B. Pfeiffer, H.L. Ravn, A. Wöhr, ISOLDE Collaboration, Z. Phys. A 340 (1991) 419.
- [21] M. Wang, G. Audi, A.H. Wapstra, F.G. Kondev, M. MacCormick, X. Xu, B. Pfeiffer, et al., Chin. Phys. C 36 (2012) 1603, <http://dx.doi.org/10.1088/1674-1137/36/12/003>.
- [22] V. Fedoseyev, G. Huber, U. Köster, J. Lettry, V.I. Mishin, H. Ravn, V. Sebastian, ISOLDE Collaboration, Hyperfine Interact. 127 (2000) 409, <http://dx.doi.org/10.1023/A:1012609515865>.
- [23] V. Bildstein, R. Gernhäuser, T. Kröll, R. Krücken, K. Wimmer, P. Van Duppen, M. Huyse, N. Patronis, R. Raabe, for the T-REX Collaboration, Eur. Phys. J. A 48 (2012) 85, <http://dx.doi.org/10.1140/epja/i2012-12085-6>.
- [24] N. Warr, J. Van de Walle, et al., Eur. Phys. J. A 49 (2013) 40, <http://dx.doi.org/10.1140/epja/i2013-13040-9>.
- [25] P. Hoff, B. Fogelberg, Nucl. Phys. A 368 (1981) 210, [http://dx.doi.org/10.1016/0375-9474\(81\)90683-7](http://dx.doi.org/10.1016/0375-9474(81)90683-7).
- [26] I.J. Thompson, Comput. Phys. Rep. 7 (1988) 167.
- [27] J.A. Tostevin, University of Surrey version of the code TWOFNR (of M. Toyama, M. Igarashi and N. Kishida) and code FRONT (*Priv. Comm.*).
- [28] H. An, C. Cai, Phys. Rev. C 73 (2006) 054605, <http://dx.doi.org/10.1103/PhysRevC.73.054605>.
- [29] A. Koning, J. Delaroche, Nucl. Phys. A 713 (2003) 231, [http://dx.doi.org/10.1016/S0375-9474\(02\)01321-0](http://dx.doi.org/10.1016/S0375-9474(02)01321-0).
- [30] J.M. Lohr, W. Haerberli, Nucl. Phys. A 232 (1974) 381, [http://dx.doi.org/10.1016/0375-9474\(74\)90627-7](http://dx.doi.org/10.1016/0375-9474(74)90627-7).
- [31] Y. Han, Y. Shi, Q. Shen, Phys. Rev. C 74 (2006) 044615, <http://dx.doi.org/10.1103/PhysRevC.74.044615>.
- [32] F.G. Perey, Phys. Rev. 131 (1963) 745, <http://dx.doi.org/10.1103/PhysRev.131.745>.
- [33] F.D. Becchetti, G.W. Greenlees, Phys. Rev. 182 (1969) 1190, <http://dx.doi.org/10.1103/PhysRev.182.1190>.
- [34] S.M. Lenzi, F. Nowacki, A. Poves, K. Sieja, Phys. Rev. C 82 (2010) 054301, <http://dx.doi.org/10.1103/PhysRevC.82.054301>.